

Soft Pomeron in the Colour Glass Condensate approach

Carlos Contreras,^{1,*} Eugene Levin,^{1,2,3,†} and Michael Sanhueza^{1,‡}

¹*Departamento de Física, Universidad Técnica Federico Santa María,
Avda. España 1680, Casilla 110-V, Valparaíso, Chile*

²*Centro Científico-Tecnológico de Valparaíso, Avda. España 1680, Casilla 110-V, Valparaíso, Chile*

³*Department of Particle Physics, School of Physics and Astronomy,
Raymond and Beverly Sackler Faculty of Exact Science, Tel Aviv University, Tel Aviv, 69978, Israel*

(Dated: March 22, 2022)

In this paper we suggest a new approach to the structure of the soft Pomeron: based on the t -channel unitarity, we expressed the exchange of the soft Pomeron through the interaction of the dipole of small size of the order of $1/Q_s(Y)$ ($Q_s(Y)$ is the saturation momentum) with the hadrons. Therefore, it is shown that the typical distances in soft processes are small $r \sim 1/Q_s(\frac{1}{2}Y)$, where $Y = \ln s$. The saturation momentum, which determines the energy dependence of the scattering amplitude is proportional to $Q_s^2(\frac{1}{2}Y) \propto \exp(\frac{1}{2}\lambda Y)$, with $\lambda \approx 0.2$, and this behaviour is in perfect agreement with phenomenological Donnachie-Landshoff Pomeron. We demonstrate that the saturation models could describe the experimental data for $\sigma_{tot}, \sigma_{el}, \sigma_{diff}$ and B_{el} . Hence our approach is a good first approximation to start discussion of the soft processes in CGC approach on the solid theoretical basis.

PACS numbers: 13.60.Hb, 12.38.Cy

Contents

I. Introduction	1
II. BFKL Pomeron in the coordinate representation	3
III. t-channel unitarity for the BFKL Pomeron	4
IV. t-channel unitarity: general case	6
V. Dressed BFKL Pomeron in proton-proton scattering	7
A. The master equation	7
B. The simple model for DIS	7
C. Realistic estimates	9
VI. Diffraction dissociation in the region of large masses	11
VII. Conclusions	14
VIII. Acknowledgements	16
References	16

I. INTRODUCTION

We believe that high energy scattering can be described in Reggeon Field Theory (RFT) of Quantum Chromodynamics (QCD), which development has led to understanding of many characteristic features of the processes at high energies, including the phenomenological application to LHC, RHIC and HERA data during the past three decades.

The basic ideas of RFT go back to pre-QCD era, when in 1967 V.N. Gribov [1] proposed his diagram technique, that is based on a very general picture and properties of high energy exchanges in a local field theory. These general ideas were assimilated to QCD and worked out over the years in many papers [2–35]. However, in spite of much work that has been done, the theoretical framework of RFT is still incomplete. Actually, we face two problems with

RFT: the first is the s -channel unitarity for dilute-dense parton system scattering, which is governed by JIMWLK¹ equation [35]; and the second one is related to the summation of the BFKL Pomeron loops [36–42].

Bearing this in mind, we cannot be surprised that RFT is not able to describe the soft interaction of hadrons at high energies. On the other hand, the Colour Glass Condensate (CGC) approach as well as its realization in RFT, leads to a new saturation scale (saturation momentum $Q_s(Y)$) which increases at large rapidities (Y). It gives us a hope that the soft interactions actually stem from sufficient short distances where we can apply RFT in QCD. Phenomenological attempts to describe the soft experimental data, based on these ideas with some additional assumptions, turn out to be rather successful (see Refs. [43, 44] and references therein).

The main building block of the Gribov Pomeron calculus is the exchange of the soft Pomeron with the Green's function:

$$G_{\mathbb{P}}(Y, Q_T) = \left(\frac{s}{s_0} \right)^{\alpha_{\mathbb{P}}(Q_T)} = e^{(\Delta - \alpha'_{\mathbb{P}} Q_T^2) Y} \quad (1)$$

where $\alpha_{\mathbb{P}}(Q_T) = \Delta - \alpha'_{\mathbb{P}} Q_T^2$ is the Pomeron trajectory and Q_T is the momentum transferred by the Pomeron.

Our goal in this paper is to build the main ingredient of the RFT such as soft Pomeron in the Pomeron calculus, using the JIMWLK evolution. Our basic idea can be illustrated using the simple Pomeron Green's function of Eq. (1). One can notice that this Green's function has the following factorization property:

$$G_{\mathbb{P}}(Y, Q_T) = G_{\mathbb{P}}(Y - y, Q_T) G_{\mathbb{P}}(y, Q_T) \quad (2)$$

for any value of y . Actually, Eq. (2) follows directly from t -channel unitarity [1] and, therefore, has a general origin and, hence, should be held in QCD. In sections II, III and IV we will show that this is a correct expectation and, indeed, we will generalize Eq. (2) to QCD. It should be noted that this generalization includes the integration over the sizes of dipoles with rapidities Y . On the other hand, the contribution of the Pomeron to hadron-hadron scattering can be written in the form:

$$N_{\mathbb{P}}(Y, Q_T) = g_h^2(Q_T) G_{\mathbb{P}}(Y, Q_T) \quad (3)$$

and using Eq. (2) we can re-write Eq. (3) as follows:

$$N_{\mathbb{P}}(Y, Q_T) = N_{\mathbb{P}}^h(Y - y, Q_T) N_{\mathbb{P}}^h(y, Q_T) \quad \text{with} \quad N_{\mathbb{P}}^h(y', Q_T) = g_h(Q_T) G_{\mathbb{P}}(y', Q_T) \quad (4)$$

In section V we will show that Eq. (4) can be generalized to QCD with $N_{\mathbb{P}}^h$, that has the meaning of the dipole scattering amplitude with the hadron. Such an amplitude can be estimated using the non-linear Balitsky-Kovchegov evolution[19]. Using the generalization of Eq. (4) we conclude that the contribution of the dressed BFKL (Balitsky, Fadin, Kuraev and Lipatov) Pomeron [2] to hadron-hadron scattering amplitude is proportional to the minimal of two saturation momenta: $Q_s^2(Y - y)$ and $Q_s^2(y)$. Choosing $y = \frac{1}{2}Y$ we obtain the largest contribution, which stems from the shortest distances, providing the best theoretical accuracy in perturbative QCD estimates. Since from high energy phenomenology $Q_s^2(y) = \exp(\lambda Y)$ with $\lambda = 0.2 - 0.25$ [45, 46], one can see that we expect the intercept of the dressed BFKL Pomeron will be $\Delta = 0.1 - 0.125$, which is close to the soft phenomenological Donnachie-Landshoff Pomeron [47] intercept. It should be pointed out, that the dressed BFKL Pomeron is quite different from the BFKL Pomeron, which has been derived from perturbative QCD in Ref. [2], since in our approach the interactions between perturbative BFKL Pomerons have been taken into account in the triple Pomeron vertex and their vertices of interaction with the hadron. These interactions result in the fact, that the short distances of about $r \sim 1/Q_s$ contribute to the soft interaction at high energies. Small but not equal to zero Δ means that the exchange of the dressed BFKL Pomeron violates the Froissart theorem [48]. The interaction between dressed Pomerons as well as their interactions with hadrons, have to be found and to be taken into account to obtain the scattering amplitude of hadron-hadron interaction. Such a difficult task is certainly out of scope of this paper and perhaps to solve this problem we will need a new theoretical input both from RFT and from non-perturbative QCD. In this paper for our estimates of the scale of such contributions we use the simple eikonal, Glauber formula [49], which restores the Froissart theorem.

In section VI we will discuss the dressed Pomeron contribution to diffractive production. In conclusions, we summarize our results and discuss the future prospects.

¹ Jalilian-Marian, Iancu, McLerran, Weigert, Leonidov and Kovner (JIMWLK) equation [21–28]

II. BFKL POMERON IN THE COORDINATE REPRESENTATION

It is well known that the scattering amplitude $N(Y; \mathbf{r}, \mathbf{R}; \mathbf{Q}_T)$ of the dipole with size r and rapidity $Y \gg 1$ with the dipole of the size R at the rest has the following form in the leading $\log(1/x)$ approximation (LLA) at high energy (see Refs. [2–4, 14]:

$$N^{\text{BFKL}}(Y; \mathbf{r}, \mathbf{R}; \mathbf{Q}_T) = \frac{rR}{16} \sum_{n=-\infty}^{\infty} \int_{-\infty}^{\infty} d\nu e^{\omega(\nu, n)Y} \frac{1}{\left(\nu^2 + \left(\frac{n-1}{2}\right)^2\right) \left(\nu^2 + \left(\frac{n+1}{2}\right)^2\right)} E_Q^{n, \nu}(r) E_Q^{n, -\nu}(R) \quad (5)$$

In Eq. (5) Q_T is the transverse momentum that is transferred by the BFKL Pomeron (see Fig. 1). One can see that the scattering amplitude can be viewed as the sum of the exchange of the reggeons whose intercepts are equal to:

$$\omega(\nu, n) = 2\bar{\alpha}_S \left(\psi(1) - \text{Re} \left\{ \psi \left(\frac{|n|+1}{2} + i\nu \right) \right\} \right); \quad (6a)$$

$$\omega(\nu, n=0) = 2\bar{\alpha}_S \left(\psi(1) - \text{Re} \left\{ \psi \left(\frac{1}{2} + i\nu \right) \right\} \right) \xrightarrow{\nu \ll 1} \omega_0 + D\nu^2 = 4 \ln 2 \bar{\alpha}_S + 14 \zeta(3) \bar{\alpha}_S \nu^2 \quad (6b)$$

where $\psi(z)$ is the Euler ψ -function (see formula **8.36** of Ref. [50]) and $\bar{\alpha}_S = \frac{N_c}{\pi} \alpha_S$. Generally speaking, $E_Q^{n, \nu}(r)$ are the Fourier images of the eigenfunction of the BFKL Hamiltonian in the coordinate space:

$$E^{n, \nu}(\rho_{10}, \rho_{20}) = (-1)^n \left(\frac{\rho_{10} \rho_{20}}{\rho_{12}} \right)^{h-\frac{1}{2}} \left(\frac{\rho_{10}^* \rho_{20}^*}{\rho_{12}^*} \right)^{\tilde{h}-\frac{1}{2}} \quad \text{with } h = \frac{n}{2} - i\nu; \quad \tilde{h} = -\frac{n}{2} - i\nu; \quad (7)$$

where $\rho_{ik} \equiv \rho_i - \rho_k$ are complex transverse coordinates. They take the form [3, 4, 14]:

$$E_Q^{n, \nu}(r) = \frac{2\pi^2}{b_{n, \nu}} \frac{1}{r} \int dz dz^* e^{\frac{i}{2}(q^* z + q z^*)} E^{n, \nu} \left(z + \frac{1}{2}\rho, z - \frac{1}{2}\rho \right) \quad (8)$$

where

$$b_{n, \nu} = \frac{2^4 i \nu \pi^3}{\frac{1}{2}|n| - i\nu} \frac{\Gamma(\frac{1}{2}|n| - i\nu + 1) \Gamma(\frac{1}{2}|n| + i\nu)}{\Gamma(\frac{1}{2}|n| + i\nu + 1) \Gamma(\frac{1}{2}|n| - i\nu)}; \quad (9)$$

The explicit form of $E_Q^{n, \nu}(r)$ have been discussed in Refs. [3, 4, 14] and for $n=0$ they take the forms:

$$E_Q^{n=0, \nu}(r) = (Q_T^2)^{i\nu} 2^{-6i\nu} \Gamma^2(1+i\nu) \left\{ J_{-i\nu} \left(\frac{q^* \rho}{4} \right) J_{-i\nu} \left(\frac{q \rho^*}{4} \right) - J_{i\nu} \left(\frac{q^* \rho}{4} \right) J_{i\nu} \left(\frac{q \rho^*}{4} \right) \right\} \quad (10)$$

In Eq. (8) - Eq. (10) we use the complex number representation for the two-dimensional vectors: $\mathbf{r} = (x, y) \rightarrow (\rho, \rho^*)$ with $\rho = x+iy$ and $\rho^* = x-iy$; and $\mathbf{Q}_T = (Q_{T,x}, Q_{T,y}) \rightarrow (q, q^*)$ with $q = Q_{T,x} + i Q_{T,y}$ and $q^* = Q_{T,x} - i Q_{T,y}$.

For $Q_T \rightarrow 0$ Eq. (5) takes a simple form (see Ref. [3] Eq. 32)

$$N^{\text{BFKL}}(Y; \mathbf{r}, \mathbf{R}; \mathbf{Q}_T \rightarrow 0) = \frac{rR}{8} \sum_{n=-\infty}^{\infty} e^{i(\varphi - \psi)n} \int_{-\infty}^{\infty} d\nu e^{\omega(\nu, n)Y} \frac{1}{\left(\nu^2 + \left(\frac{n-1}{2}\right)^2\right) \left(\nu^2 + \left(\frac{n+1}{2}\right)^2\right)} \left(\frac{r^2}{R^2} \right)^{i\nu} \quad (11)$$

where φ and ψ are angles with the x -axis of \mathbf{r} and \mathbf{R} , respectively.

Actually Eq. (5) and Eq. (11) give the scattering amplitude of two dipoles, which satisfies the initial condition:

$$N^{\text{BFKL}}(Y=0; \mathbf{r}, \mathbf{R}; \mathbf{b}) = N^{\text{BA}}(\mathbf{r}, \mathbf{R}; \mathbf{b}) = 2\pi^2 \ln^2 \left(\frac{r^2 R^2}{\left(\mathbf{b} + \frac{1}{2}(\mathbf{r} - \mathbf{R})\right)^2 \left(\mathbf{b} - \frac{1}{2}(\mathbf{r} - \mathbf{R})\right)^2} \right) \quad (12)$$

where N^{BA} is the scattering amplitude due to exchange of two gluons between the dipoles with sizes r and R at the impact parameter \mathbf{b} (see Refs. [3, 51]).

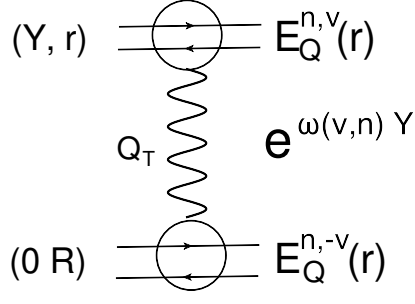


FIG. 1: The general representation of the BFKL Pomeron Green function for the scattering of the dipole with rapidity Y and size r with the dipole with size R , which is at the rest. b is the impact parameter of this amplitude. Q_T is the transverse momentum transferred by the Pomeron.

The scattering amplitudes of Eq. (5) and Eq. (11) can be re-written in more general form:

$$N^{\text{BFKL}}(Y; \mathbf{r}, \mathbf{R}; \mathbf{Q}_T) = \sum_{n=-\infty}^{n=\infty} \int_{-\infty}^{\infty} d\nu N_{in}(n, \nu) G_Q^{n,\nu}(\mathbf{r}, \mathbf{R}; Y) \quad (13)$$

where

$$G_Q^{n,\nu}(\mathbf{r}, \mathbf{R}; Y) = e^{\omega(\nu,n)Y} r E_Q^{n,\nu}(r) R E_Q^{n,-\nu}(R) \quad (14)$$

is the Green's function of the BFKL Pomeron with the intercept $\omega(\nu, n)$ (see Fig. 1). $N_{in}(n, \nu)$ have to be found from the initial condition for the scattering amplitude at $Y = 0$.

III. T-CHANNEL UNITARITY FOR THE BFKL POMERON

The BFKL Pomeron is derived in leading logarithmic approximation (LLA) of perturbative QCD using t and s channel unitarity constraints [2, 9]. The s -channel means that²

$$\text{Im}_s N(Y, r, R, Q_T = 0) = \sum_n \left| N(2 \rightarrow n; \{r_i\}) \right|^2 \prod_{i=2}^n d^2 r_i \quad (15)$$

where $N(2 \rightarrow n; \{r_i\})$ is the amplitude of production of n dipoles.

The BFKL Pomeron satisfies also the t -channel unitarity, which in the channel where $t = -Q_T^2 > 0$ is the energy has the same form as Eq. (15):

$$\text{Im}_t N(Y, r, R, Q_T) = \sum_n \left| N(2 \rightarrow n; \{k_i\}) \right|^2 \prod_{i=2}^n \frac{d^2 k_i}{(2\pi)^2} \quad (16)$$

where $N(2 \rightarrow n; \{k_i\})$ is the amplitude of the production of n gluons with the transverse momenta k_i . However, it is shown [2], that t -channel unitarity, analytically continued to the s -channel, can be re-written as the integration over two reggeized gluons (see Fig. 2-a) and takes the form³:

$$G^{\text{BFKL}}(Y, Q_T, r, R) = \int \frac{d^2 k_T}{(2\pi)^2} G^{\text{BFKL}}(Y - y', Q_T, r, k_T) G^{\text{BFKL}}(y', Q_T, R, k_T) \quad (17)$$

where

² For the sake of simplicity we write this constraint at $Q_T = 0$.

³ Eq. (17) was first written in Refs. [5, 9].

$$G^{\text{BFKL}}(Y - y', Q_T, r, r') = r'^2 \int \frac{d^2 k_T}{(2\pi)^2} e^{i\mathbf{k}_T \cdot \mathbf{r}'} G^{\text{BFKL}}(Y - y', Q_T, r, k_T) \quad (18)$$

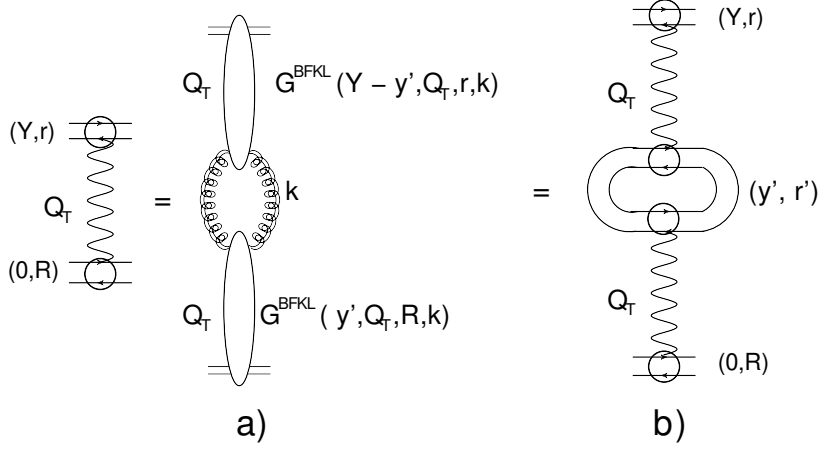


FIG. 2: t -channel unitarity for the BFKL Pomeron. The double helix lines denote the reggeized gluons.

Eq. (17) can be re-written through $G^{\text{BFKL}}(Y - y', r, r', Q_T)$ in the form (see Fig. 2-b):

$$G^{\text{BFKL}}(Y, Q_T, r, R) = \frac{1}{4\pi^2} \int \frac{d^2 r'}{r'^4} G^{\text{BFKL}}(Y - y', Q_T, r, r') G^{\text{BFKL}}(y', Q_T, r', R) \quad (19)$$

The factor $1/4\pi^2$ in Eq. (19) we will discuss below. First, let us show that Eq. (19) holds for the Green's function of Eq. (14). Using the orthogonality of $E_Q^{n,\mu}$ [14], viz.:

$$\frac{1}{4\pi^2} \int \frac{d^2 r}{r^2} E_Q^{n,-\nu}(r) E_Q^{n,\mu}(r) = \delta(\nu - \mu) \quad (20)$$

One can see that

$$G_Q^{n,\nu}(r, R; Y) = \frac{1}{4\pi^2} \int \frac{d^2 r'}{r'^4} G_Q^{n,\nu}(r, r'; Y - y') G_Q^{n,\nu}(r', R; y') \quad (21)$$

At high energies the most contribution stems from $n = 0$ Green's function and Eq. (19) can be demonstrated directly from Eq. (11) at $Q_T \rightarrow 0$:

$$G^{\text{BFKL}}(Y; \mathbf{r}, \mathbf{R}; \mathbf{Q}_T \rightarrow 0) = 2rR \int_{-\infty}^{\infty} d\nu e^{\omega(\nu,0)Y} \left(\frac{r^2}{R^2} \right)^{i\nu} \quad (22)$$

Eq. (19) can be re-written as follows:

$$\begin{aligned} G^{\text{BFKL}}(Y, r, R, Q_T) &= \frac{1}{(2\pi)^2} \int \frac{d^2 r'}{r'^4} \left\{ 2r r' \int_{-\infty}^{\infty} d\nu e^{\omega(\nu,0)(Y-y')} \left(\frac{r^2}{r'^2} \right)^{i\nu} \right\} \left\{ 2r' R \int_{-\infty}^{\infty} d\nu' e^{\omega(\nu',0)y'} \left(\frac{r'^2}{R^2} \right)^{i\nu'} \right\} \\ &= 2rR \left\{ \int_{-\infty}^{\infty} d\nu e^{\omega(\nu,0)(Y-y')} (r^2)^{i\nu} \right\} \delta(\nu - \nu') \left\{ \int_{-\infty}^{\infty} d\nu' e^{\omega(\nu',0)y'} \left(\frac{1}{R^2} \right)^{i\nu'} \right\} \\ &= 2rR \int_{-\infty}^{\infty} \frac{d\nu}{2\pi} e^{\omega(\nu,0)Y} \left(\frac{r^2}{R^2} \right)^{i\nu} \end{aligned} \quad (23)$$

Note that we checked in Eq. (23) the numerical factor $1/4\pi^2$. Actually, Eq. (23) holds for not only $n = 0$ but for all n .

Eq. (19) can be re-written in the impact parameter representation in the form:

$$G^{\text{BFKL}}(Y, \mathbf{r}, \mathbf{R}, \mathbf{b}) = \frac{1}{4\pi^2} \int \frac{d^2 r'}{r'^4} \int d^2 b' G^{\text{BFKL}}(Y - y', \mathbf{r}, \mathbf{r}', \mathbf{b} - \mathbf{b}') G^{\text{BFKL}}(y', \mathbf{r}', \mathbf{R}, \mathbf{b}') \quad (24)$$

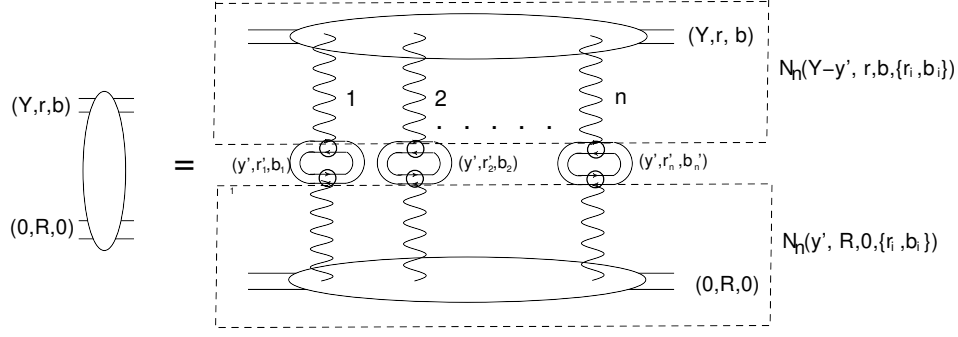


FIG. 3: t -channel unitarity for a general scattering amplitude in the BFKL Pomeron calculus.

IV. T-CHANNEL UNITARITY: GENERAL CASE

The t -channel unitarity constraints for the dipole-dipole amplitude can be re-written in a general form in the framework of the BFKL Pomeron calculus using Eq. (24) (see Fig. 3):

$$N(Y, \mathbf{r}, \mathbf{R}, \mathbf{b}) = \sum_{n=1}^{\infty} \frac{(-1)^{n-1}}{n!} \int \frac{d^2 r_i d^2 b_i}{4\pi^2} \frac{1}{r_i^4} N_n(Y - y', \mathbf{r}, \mathbf{b}; \{\mathbf{r}_i, \mathbf{b}_i\}) N_n(y', \mathbf{R}, \mathbf{0}; \{\mathbf{r}_i, \mathbf{b}_i\}) \quad (25)$$

where $N_n(Y - y', \mathbf{r}, \mathbf{b}; \{\mathbf{r}_i, \mathbf{b}_i\})$ is the amplitude of the production of n BFKL Pomerons each of which produces the dipole with size r_i at the impact parameters b_i . $Y - y'$ is the rapidity between the initial dipole r and produced dipoles r_i .

Eq. (25) is a modification of the MPSI⁴ approach [8, 52] in which we integrated over the sizes of the dipoles in the dipole-dipole scattering amplitudes at low energies using the properties of the BFKL Pomeron. This equation can be useful in the case if we know the amplitudes N_n . For example in Ref. [29] it is shown that in the kinematic region $Y - y' \leq y_{\max}$ and $y' \leq y_{\max}$ ($y_{\max} = \frac{1}{\omega_0} \ln \left(\frac{1}{\alpha_s^2} \right)$) N_n are given by the Balitsky-Kovchegov cascade (see Fig. 4). In this case Eq. (25) allows us to sum the large Pomeron loops as it is shown in Fig. 4. Eq. (25) can be re-written in this case in the following form [53, 54]:

$$N(Y, r, R, b) = \sum_{n=1}^{\infty} \frac{(-1)^{n+1}}{n!} \int \prod_{i=1}^n \frac{1}{4\pi^2} \frac{d^2 r_i d^2 b_i}{r_i^4} \frac{\delta}{\delta u_i} Z(Y - y'; \{u_i\}) \Big|_{u_i=1} \frac{\delta}{\delta u'_i} Z(y'; \{u'_i\}) \Big|_{u'_i=1} \quad (26)$$

where the generating functional $Z(Y\{u_i\})$ has been discussed in Refs. [9, 39].

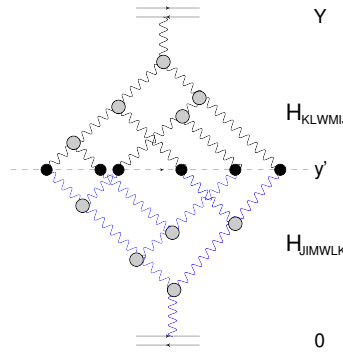


FIG. 4: The BFKL cascades, which are described by H_{JIMWLK} and by H_{KLWMIJ} (see Ref. [29]). The wavy lines denote the BFKL Pomerons. The gray circles are the triple Pomeron vertex while the black circles denote $\frac{1}{4\pi^2} \int d^2 r_i d^2 b_i \frac{1}{r_i^4}$.

⁴ Mueller, Patel, Salam and Iancu approach.

In the next section we will give another example of using Eq. (25).

V. DRESSED BFKL POMERON IN PROTON-PROTON SCATTERING

A. The master equation

Our main idea is to use Eq. (25) to estimate the proton-proton scattering. We believe that for real estimates we need to find how to sum all Pomeron diagrams including summing of the Pomeron loops. In spite of some progress in this direction [36–42] we are still far away from the solid theoretical approach both for dilute-dilute parton system scattering and for dense-dense system interaction. The example of the first one is the hadron-hadron collisions at high energies while for the second is the nucleus-nucleus scattering. In this paper we wish to realize a more restricted goal: to build the first approximation to hadron-hadron and/or nucleus-nucleus collisions. We propose the dressed Pomeron contribution, which is shown in Fig. 5, as the first approximation. In other words, we wish to introduce not the exchange of the BFKL Pomeron as the first approximation but we suggest to sum all Pomeron diagrams that contribute to the vertex for interaction of the BFKL Pomeron with the hadron (see Fig. 5).

We can see that the interaction of the BFKL Pomeron with the proton is known from the DIS data and we have numerous attempts to describe this interaction using the Balitsky-Kovchegov parton cascade [45, 56–70]. Therefore, we can develop a model for the vertex.

Our master equation is shown in Fig. 5 and has a simple form:

$$N_p^p(Y, b) = \frac{1}{4\pi^2} \int \frac{d^2r' d^2b'}{r'^4} N_p(Y - y', \mathbf{r}', \mathbf{b} - \mathbf{b}') N_p(y', \mathbf{r}', \mathbf{b}') \quad (27)$$

where N_p is the amplitude that can be found from the DIS since all observable in these processes can be expressed through the following amplitudes [51]:

$$N(Q, Y; b) = \int \frac{d^2r}{4\pi} \int_0^1 dz |\Psi_{\gamma^*}(Q, r, z)|^2 N_p(r, Y; b) \quad (28)$$

Note, that the wave functions are known at least at large values of Q . One can see that integral over r in Eq. (27) converges both at $r \rightarrow 0$ and at large $r \rightarrow \infty$. Indeed, at $r' \rightarrow 0$ $N_p(Y, r) \propto r^2$ leading to the final integral in the region of small r . At large distances $N_p(Y, r) \rightarrow 1$ and, therefore, the integral is rapidly converges at large distances.

Hence we expect that the typical r' is about of $1/Q_s$, where Q_s is the saturation scale. Bearing this in mind we expect that the dressed Pomeron will behave as $Q_s^2(\frac{1}{2}Y)$ (for $y' = \frac{1}{2}Y$). Therefore, the dressed Pomeron has the power-like behaviour with intercept $\frac{1}{2}\lambda$ if $Q_s^2(Y) \propto \exp(\lambda Y)$. Since the phenomenological value of $\lambda = 0.2 - 0.3$ we see that the value of the intercept is about $0.1 - 0.15$ in a good agreement with high energy phenomenology.⁵ It should be stressed that this estimate demonstrates that the typical values of r' is rather small ($r' \sim 1/Q_s$). Therefore, we can safely apply CGC approach for these calculations and, hence, Eq. (27) gives for the first time an estimate for soft Pomeron on the solid theoretical basis. One can see that this estimate of the typical distances is valid for the general Eq. (25), making the approach theoretically very attractive.

B. The simple model for DIS

For better understanding of Eq. (27) we model the scattering amplitude $N_p(y', \mathbf{r}', \mathbf{b})$ in the following way:

$$N_p(y, \mathbf{r}, \mathbf{b}) = a \left(1 - \exp\left(-\tau^{\tilde{\gamma}} e^{-\frac{b^2}{B}}\right) \right) + a \frac{\tau^{\tilde{\gamma}} e^{-\frac{b^2}{B}}}{1 + \tau^{\tilde{\gamma}} e^{-\frac{b^2}{B}}} \quad (29)$$

Eq. (29) leads to the scattering amplitude $N_p(y', \mathbf{r}', \mathbf{b}) = \tau^{\tilde{\gamma}} e^{-\frac{b^2}{B}}$ for $\tau = r^2 Q_0^2 \exp(\lambda y) \ll 1$. Comparing this behavior with the scattering amplitude in the vicinity of the saturation scale [55] we obtain that

⁵ We will discuss this behaviour below in more details.

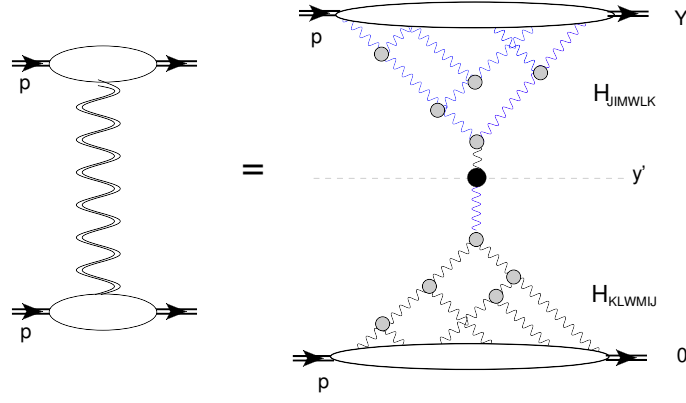


FIG. 5: The contribution of the dressed Pomeron to the proton-proton scattering. The Balitsky - Kovchegov cascades are described by H_{JIMWLK} and by H_{KLWMIJ} (see Ref. [29]). The wavy lines denote the BFKL Pomerons. The gray circles are the triple Pomeron vertex while the black circle denotes $\frac{1}{4\pi^2} \int d^2r d^2b_i \frac{1}{r^4}$. The double wavy line describes the dressed Pomeron.

$\tau^{\bar{\gamma}} = N_0 (r^2 Q_s^2(y, b=0))^{\bar{\gamma}}$ with $Q_s^2(y, b) = Q_0^2 \exp(\lambda y) e^{-\frac{b^2}{\bar{\gamma} B}}$. For $\tau > 1$ Eq. (29) with $a=0.65$ gives the good parameterization of the solution to the non-linear Balitsky-Kovchegov (BK) equation for the leading twist [42]. For the total cross section Eq. (27) takes the form:

$$\sigma_{\text{tot}}^{pp} = \frac{2}{4\pi^2} \int d^2r \left(\int d^2b N_p(y', \mathbf{r}, \mathbf{b}) \right)^2 / r^4 \quad (30)$$

The integral over b can be taken explicitly, viz.:

$$\int d^2b N_p(y, \mathbf{r}, \mathbf{b}) = \pi B \left((1-a) \ln(\tau^{\bar{\gamma}} + 1) + a(\ln(\tau^{\bar{\gamma}}) + \Gamma(0, \tau^{\bar{\gamma}})) \right) \quad (31)$$

Using Eq. (31) we can re-write Eq. (30) as follows:

$$\sigma_{\text{tot}}^{pp} = \frac{\pi}{2} B^2 N_0^{\frac{1}{\bar{\gamma}}} Q_0^2 e^{\frac{1}{2}\lambda y} \int d\tau \left((1-a) \ln(\tau^{\bar{\gamma}} + 1) + a(\ln(\tau^{\bar{\gamma}}) + \Gamma(0, \tau^{\bar{\gamma}})) \right)^2 / \tau^2 \quad (32)$$

For $a = 0.65$ and $\bar{\gamma} = 0.63$, which stems from the leading order estimates, the integral over τ is equal to 4.96. Hence we have for the cross section:

$$\sigma_{\text{tot}}^{pp} = \frac{4.96\pi}{2} B^2 N_0^{\frac{1}{\bar{\gamma}}} Q_0^2 e^{\frac{1}{2}\lambda y} \quad (33)$$

The values of λ, N_0, B and Q_0^2 have been estimated in the variety of models [56–74] which describe the experimental data on DIS from HERA. These models lead to $B = 5.5 \text{ GeV}^{-2}$, which can be fixed from the production of J/Ψ meson in DIS; to $N_0 = 0.23 - 0.34$ and of $\lambda = 0.2 - 0.25$. In the most models $Q_0^2 \approx 0.2 \text{ GeV}^2$. Using these values for parameters we have $\sigma_{\text{tot}}^{pp} = 39 \text{ mb}$ instead of the experimental value of $\sigma_{\text{tot}}^{pp} = 62 \text{ mb}$ at $W = 540 \text{ GeV}$. However, the saturation model in the next-to-leading order (see Ref. [72] for example) lead to larger values of Q_0^2 .

In Fig. 6 we plot the values for the total cross section for proton-proton scattering (solid line) that come from Eq. (29) for two values of $Q_0^2 = 0.2 \text{ GeV}^2$ and $Q_0^2 = 0.4 \text{ GeV}^2$.

In Fig. 7 we show the dependence of the dressed Pomeron of Eq. (29) on Y and y' using this model. From Fig. 7 one can see that the contribution of the dressed Pomeron depends on the choice of y' . However, this dependence is not very steep. As it is shown in Ref. [52] the minimal corrections appear at $y' = \frac{1}{2}Y$, which we will use in our further estimates.

It should be stressed that Fig. 6 is the first estimates of the cross section for the soft process that has been made in CGC approach on solid theoretical ground. We will present the more reliable estimates based on Eq. (27) without using the simplified models. However, these first estimates show us that the approach with the dressed Pomeron can

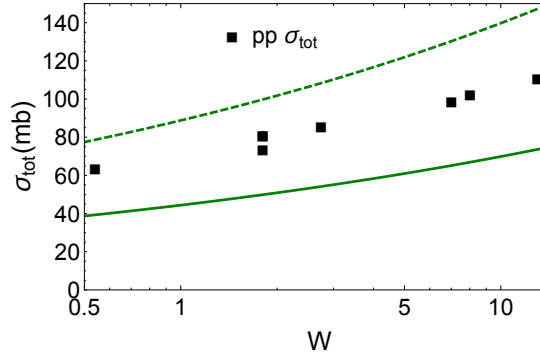


FIG. 6: σ_{tot} versus W . The curves are calculated, using Eq. (30)-Eq. (33). The solid curve corresponds to $Q_0^2 = 0.2 \text{ GeV}^2$ while the dashed one is for $Q_0^2 = 0.4 \text{ GeV}^2$. The data are taken from Refs. [75, 76]. $\lambda = 0.196$, $N_0 = 0.3$, $B = 11 \text{ GeV}^{-2}$.

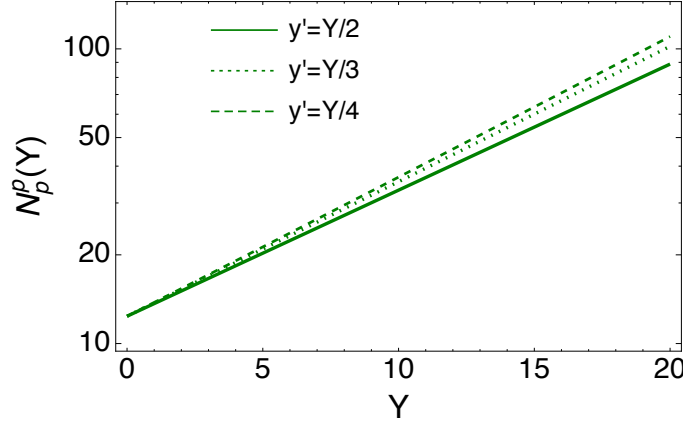


FIG. 7: The dressed Pomeron at $b = 0$ versus Y at different values of y' . The parameters of Eq. (29) are taken from Ref. [71]: $N_0 = 0.34$, $\lambda = 0.195$, $Q_0^2 = 0.145 \text{ GeV}^2$ and $m = 0.75 \text{ GeV}$. The saturation scale is parameterized as $Q_s(Y, b) = Q_0^2 \exp(\lambda Y) S(b)$ with $S(b) = (mb K_1(mb))^{\frac{1}{\bar{\gamma}}}$.

be rather useful. The simple model led to the cross section which describes the energy behavior of the experimental data. The values of the parameters have large dispersions, but for the first estimate we believe, that we will be able to obtain a good agreement with the data of the cross section values. However, we cannot reproduce the values and energy dependence of σ_{el} and B_{el} from Eq. (36b) and Eq. (36c). We will come back to this problem after making more reliable estimates beyond the simple model.

C. Realistic estimates

At first sight for the amplitude $N_p(y', r', b')$ in Eq. (27) we can use the non-linear BK equation [19]. However, since the CGC approach suffers the severe theoretical problem of violating the Froissart theorem at large impact parameters (b) [77–80], we have to build models which give the scattering amplitude with exponential decrease at large b . All these models use the theoretically solid behaviour of the scattering amplitude in the vicinity of the saturation scale ($\tau = r^2 Q_s^2(y, b) \sim 1$) [55]:

$$N_p(y, r, b) = N_0 (r^2 Q_s^2(y, b))^{\bar{\gamma}} \quad (34)$$

with $\bar{\gamma} = 0.63$ in the leading order of perturbative QCD.

However, for the b -dependence of the saturation scale the phenomenological $\exp(-\mu b)$ or $\exp(-b^2/B)$ behaviour is taken instead of the power-like decrease, that follows from the BK equation. For $\tau > 1$ it is assumed the geometric scaling behaviour of the scattering amplitude [81–83], which leads to $N_p = N_p(\tau)$. We need to use BK equation to

find this function. However, only in Refs. [71, 72, 74] such procedure has been developed. In other models the rough approximation to the BK equation has been applied. For realistic estimates we chose the model of Ref. [74], which includes all theoretical ingredients from the CGC approach (see Ref. [84]) and introduces the exponential decrease of the saturation scale with b which follows from the Froissart theorem [48]. In Fig. 8 we plot our estimates from Eq. (30) for all sets of parameters of Ref. [74], which demonstrates that the values of the cross sections can be close to the experimental ones. One can see that sets 1 and 3 describe the experimental data while all others leads to the cross section, which larger or smaller than the experimental one. Such large dispersion of the estimates is mostly related to the energy dependence of the saturation scale, which leads to different values of the typical distances in the integral over r in Eq. (30).

The large differences between the estimates of the model of Ref. [74] and of Ref. [70] and/or Eq. (33) stems from the fact that the value of Q_0^2 in Ref. [74] is about 1 GeV^2 being almost 3-5 times larger than that in Fig. 6.

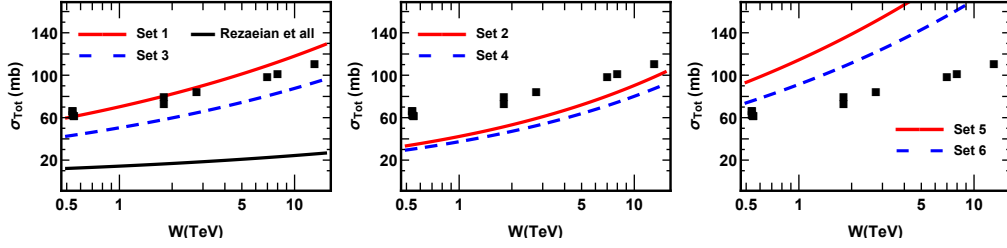


FIG. 8: σ_{tot} versus W from Eq. (30) for all sets of Ref. [74]. The solid black line corresponds to the saturation model of Ref. [70].

It should be noted that Eq. (30) cannot describe the energy dependence of the slope for differential elastic cross section as well as the value of σ_{el} . Bearing this in mind we made the estimates for the shadowing corrections using the eikonal formula:

$$A^{pp}(Y, b) = i \left(1 - \exp(-N_p^p(Y, b)) \right) \quad (35)$$

The observables can be expressed through the amplitude of Eq. (35) in the following form:

$$\sigma_{tot}(Y) = 2 \int d^2b \text{Im} A^{pp}(Y, b); \quad (36a)$$

$$\sigma_{el}(Y) = \int d^2b |A^{pp}(Y, b)|^2; \quad (36b)$$

$$B_{el} = \frac{1}{2} \int b^2 d^2b \text{Im} A^{pp}(Y, b) \bigg/ \int d^2b \text{Im} A^{pp}(Y, b); \quad (36c)$$

In Fig. 9 we compare our estimates, using Eq. (35) - Eq. (36c) for all six sets of parameterization of Ref. [74]. Even a brief sight at Fig. 9 shows the wide spreading of the values for the observables. This large dispersion of the predictions supports the idea that the DIS data is not enough for fixing the parameters of the models. On the other hand, one can conclude that we are able to describe both the soft experimental data and DIS. In Fig. 9 sets 5 and 6 describe the data quite well. It is interesting to note that both these sets introduce the shrinkage of the diffraction peak due to the energy dependence of the impact parameter distribution for the saturation scale (see, for example, Refs. [85, 86]).

It worthwhile mentioning that Eq. (35) is written as the example of possible shadowing corrections just for understanding the scale of the effect. As has been discussed in the introduction the theoretical approach to these correction is still in the embryonic stage. However, applying the t-channel unitarity in its general form (see Fig. 3) we see that all Pomerons (dipoles at rapidity y') enter at the same typical sizes $r = 1/Q_s$. Hence, we can try to treat the shadowing corrections in the toy model: the QCD approach in which all dipoles have the same size [9, 18, 29, 87–89].

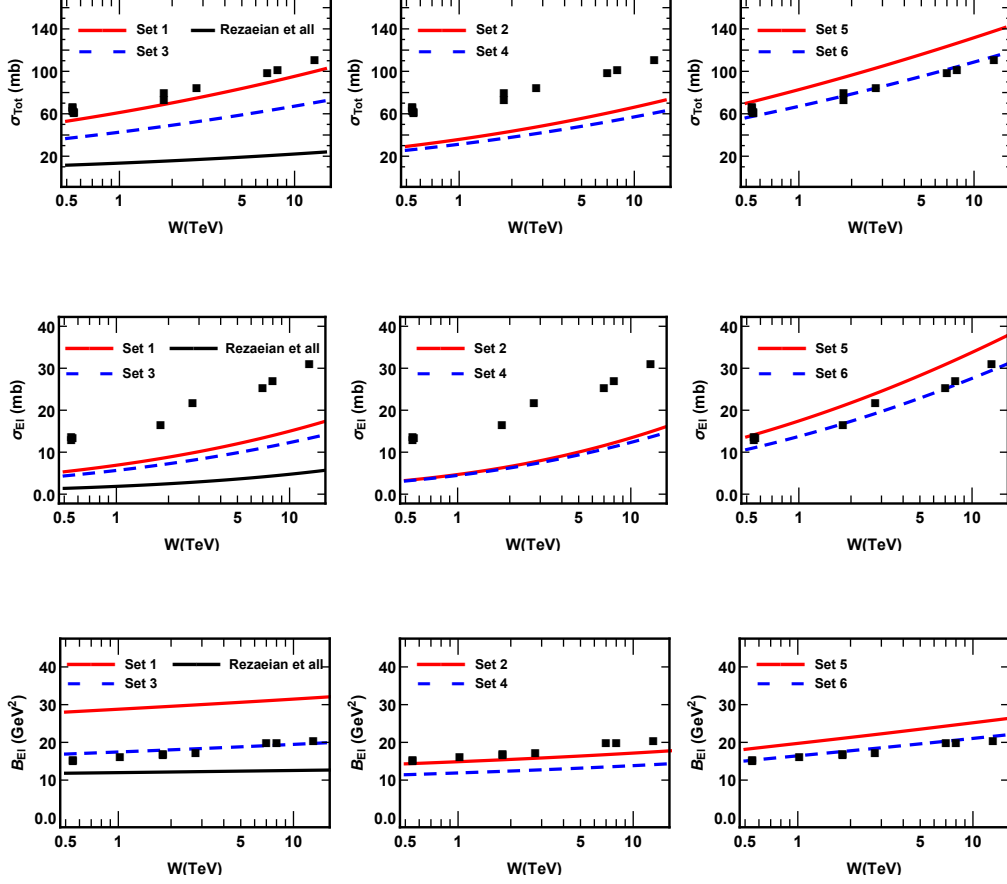


FIG. 9: Comparison of σ_{tot} , σ_{el} and B_{el} with the experimental data for all sets of parameterization of Ref. [74]. The solid black line corresponds to the saturation model of Ref. [70]. The data are taken from Refs. [75, 76].

VI. DIFFRACTION DISSOCIATION IN THE REGION OF LARGE MASSES

In this section we are going to study the cross section of the single diffractive dissociation. The physical picture of the process we are going to consider is the following: in DIS the virtual photon interacts with the hadron or nucleus breaking up into hadrons and jets in the final state. At the same time the target hadron (nucleus) remains intact. The particles produced as a result of the hadron breakup do not fill the whole rapidity interval, leaving a rapidity gap between the target and the slowest produced particle as a function of the invariant mass of the produced hadrons M . The diffractive production of hadrons with large mass is intimately related to the triple Pomeron diagram which is shown in Fig. 10. The three Pomeron vertex can be found from the Balitsky-Kovchegov [19] non-linear equation:

$$\begin{aligned}
 \frac{\partial}{\partial Y} N(\mathbf{x}_{10}, \mathbf{b}, Y; R) = & \\
 \bar{\alpha}_S \int \frac{d^2 \mathbf{x}_2}{2\pi} K(\mathbf{x}_{02}, \mathbf{x}_{12}; \mathbf{x}_{10}) & \left(N\left(\mathbf{x}_{12}, \mathbf{b} - \frac{1}{2}\mathbf{x}_{20}, Y; R\right) + N\left(\mathbf{x}_{20}, \mathbf{b} - \frac{1}{2}\mathbf{x}_{12}, Y; R\right) - N(\mathbf{x}_{10}, \mathbf{b}, Y; R) \right. \\
 & \left. - N\left(\mathbf{x}_{12}, \mathbf{b} - \frac{1}{2}\mathbf{x}_{20}, Y; R\right) N\left(\mathbf{x}_{20}, \mathbf{b} - \frac{1}{2}\mathbf{x}_{12}, Y; R\right) \right)
 \end{aligned} \tag{37}$$

where $\mathbf{x}_{ik} = \mathbf{x}_i - \mathbf{x}_k$ and $\mathbf{x}_{10} \equiv \mathbf{r}$, $\mathbf{x}_{20} \equiv \mathbf{r}'$ and $\mathbf{x}_{12} \equiv \mathbf{r} - \mathbf{r}'$. Y is the rapidity of the scattering dipole and \mathbf{b} is the impact factor. $K(\mathbf{x}_{02}, \mathbf{x}_{12}; \mathbf{x}_{10})$ is the kernel of the BFKL equation which has the following form:

$$K(\mathbf{x}_{02}, \mathbf{x}_{12}; \mathbf{x}_{10}) = \frac{x_{10}^2}{x_{12}^2 x_{02}^2} \quad (38)$$

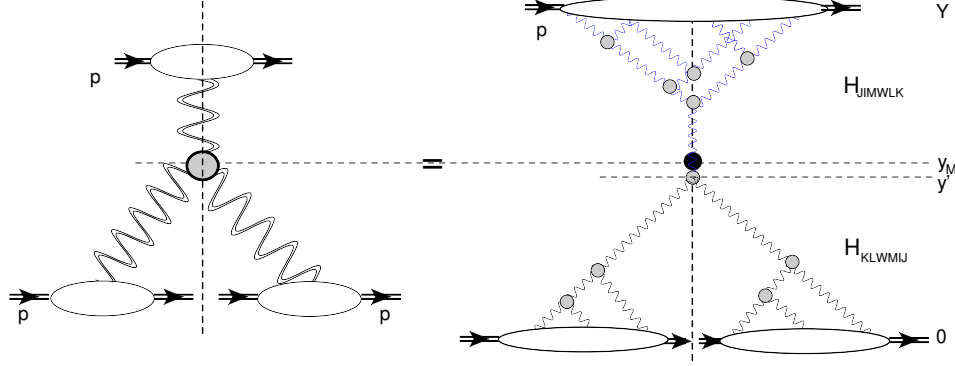


FIG. 10: The contribution of the dressed Pomeron to the diffraction production of large mass in the proton-proton scattering. The Balitsky-Kovchegov cascades are described by H_{JIMWLK} and by H_{KLWMIJ} (see Ref. [29]). The wavy lines denote the BFKL Pomerons. The gray circles are the triple Pomeron vertex while the black circle denotes $\frac{1}{4\pi^2} \int d^2 r_i d^2 b_i \frac{1}{r_i^4}$. The double wavy line describes the dressed Pomeron. $Y - y_M = \ln M^2$, where M is the mass of produced hadrons. The vertical dashed line denotes the cut Pomeron.

The last term of Eq. (37) gives the triple Pomeron contribution. Using Eq. (27) we can re-write the equation given by Fig. 10 in the following analytical form:

$$\begin{aligned} \frac{d\sigma_{sd}(Y, y_M)}{dy_M} &= \frac{2}{4\pi^2} \int \frac{d^2 r}{r^2} \int d^2 b N_p(Y - y_M, \mathbf{r}, \mathbf{b}) \\ &\times \left\{ \bar{\alpha}_S \int d^2 b' \int \frac{d^2 r'}{2\pi} \frac{1}{r'^2} N_p\left(y_M, \mathbf{r}', \mathbf{b}' - \frac{1}{2}(\mathbf{r} - \mathbf{r}')\right) \frac{1}{(\mathbf{r} - \mathbf{r}')^2} N_p\left(y_M, \mathbf{r} - \mathbf{r}', \mathbf{b}' - \frac{1}{2}\mathbf{r}'\right) \right\} \end{aligned} \quad (39)$$

where $Y - y_M = \ln M^2$ where M is the mass of produced hadrons (see Fig. 10).

In Eq. (39) the typical values of $r(r')$ are $r \sim 1/Q_s(Y - Y_M, b)$ and $r' \sim 1/Q_s(Y_M, b')$. For understanding the dependence on y_M we can consider two different cases.

1. $Q_s(Y - Y_M, b) \gg Q_s(Y_M, b')$

In this case we see that $r \ll r'$ and the integral over r' takes the form:

$$I(r) \equiv \int_{r' > r} \frac{d^2 r'}{2\pi} \frac{1}{r'^4} N(y_M, \mathbf{r}', \mathbf{b}') N(y_M, \mathbf{r}', \mathbf{b}') \propto Q_s^2(y_M, b') \quad (40)$$

where we consider that $b \sim 1/\mu \gg r(r') \sim 1/Q_s$. Hence, we infer that the rapidity dependence of $\frac{d\sigma_{sd}(Y, y_M)}{dy_M}$ is $\frac{d\sigma_{sd}(Y, y_M)}{dy_M} \propto \int d^2 b' Q_s^2(y_M, b')$. However, it is not correct. Indeed, the integration over r takes the form

$$\int \frac{d^2 r}{r^2} N_p(Y - y_M, \mathbf{r}, \mathbf{b}) I(r) \quad (41)$$

This integral converges at large r only due to a decrease of function $I(r)$ which can occur only for $r > 1/Q_s(Y_M, b)$. Therefore, in the region of $1/Q_s(Y_M, b) > r > 1/Q_s(Y - Y_M, b)$ we have a logarithmic integral which leads to the contribution:

$$\int \frac{d^2 r}{r^2} N_p(Y - y_M, \mathbf{r}, \mathbf{b}) I(r) = C_{r' > r} + \ln\left(\frac{Q_s(Y - Y_M, b)}{Q_s(Y_M, b)}\right) = C_{r' > r} + \lambda(Y - 2y_M) \quad (42)$$

Therefore, we expect that the contribution to the diffraction production from this kinematic region has a general form:

$$\frac{d\sigma_{sd}(Y, y_M; r', r)}{dy_M} \propto Q_s^2(y_M, b') \left(C_{r' > r} + \lambda(Y - 2y_M) \right) \quad (43)$$

$$2. \quad Q_s(Y - y_M, b) \ll Q_s(Y_M, b')$$

In this kinematic region the typical $r \gg r'$ and we obtain the integral over r in the form:

$$\int \frac{d^2r}{2\pi} \frac{1}{r^4} N_p(Y - y_M, \mathbf{r}, b) N_p(y_M, \mathbf{r}, b') \propto Q_s^2(Y - y_M, b) \quad (44)$$

leading to $\frac{d\sigma_{sd}(Y, y_M)}{dy_M} \propto \int d^2b Q_s^2(Y - y_M, b)$. Note, that $N(y_M, \mathbf{r}, b') \rightarrow 1$ in this kinematic region. Repeating the same estimates as in the case 1 for integration over r' we conclude that

$$\frac{d\sigma_{sd}(Y, y_M; r', r)}{dy_M} \propto Q_s^2(Y - y_M, b') \left(C_{r > r'} - \lambda(Y - 2y_M) \right) \quad (45)$$

From Eq. (43) and Eq. (45) we conclude that $\frac{d\sigma_{sd}(Y, y_M; r', r)}{dy_M}$ has maximum in the region of $y_M \approx \frac{1}{2}Y$. It is easy to see that $C_{r > r'} > C_{r' > r}$ and hence the maximum is shifted to $y_M > \frac{1}{2}Y$.

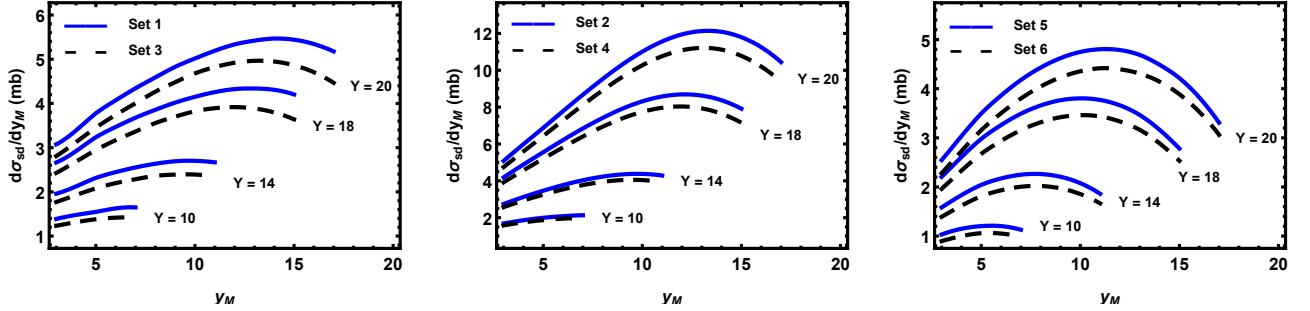


FIG. 11: Cross section of the single diffraction production $\frac{d\sigma_{sd}(Y, y_M)}{dy_M}$ versus y_M at different values of y for sets 1-6 of Ref. [74].

Hence, we can expect that

$$\sigma^{diff} = \int dy_M \frac{d\sigma_{sd}(Y, y_M)}{dy_M} \propto \int d^2b Q_s^2\left(\frac{1}{2}Y, b\right) \left(\text{Const} + \lambda Y \right) \quad (46)$$

In Fig. 11 we plot the estimates for $\frac{d\sigma_{sd}(Y, y_M)}{dy_M}$ in different parameterizations of Ref. [74]. At not very large Y the cross section increases with the increase of rapidity gap ($y_{\text{gap}} = Y - y_M$), which agrees with the result of the traditional triple pomeron description of the diffractive dissociation. However, as y_{gap} gets very high and reaches the values of rapidity at saturation, the cross section reaches a maximum and starts decreasing. One can see that distribution over y_M has a maximum in the region of $y_M \approx \frac{1}{2}Y$, which has been expected from the qualitative discussions above. It should be mentioned that such a maximum follows from the non linear evolution equation for diffractive dissociation processes in QCD [11].

In Fig. 12 the values of $\sigma^{diff} = \int_{y_0}^{Y-y_0} dy_M \frac{d\sigma_{sd}(Y, y_M)}{dy_M}$ are plotted. The value of y_0 is chosen $y_0 = 3$, which reflects our belief that we can consider the Pomeron exchange starting with rapidity $\geq y_0$. One can see that the Y dependence in this figure reproduces the estimates of Eq. (46). On the other hand, the values turn out to be very large and, hence, the shadowing corrections are needed.

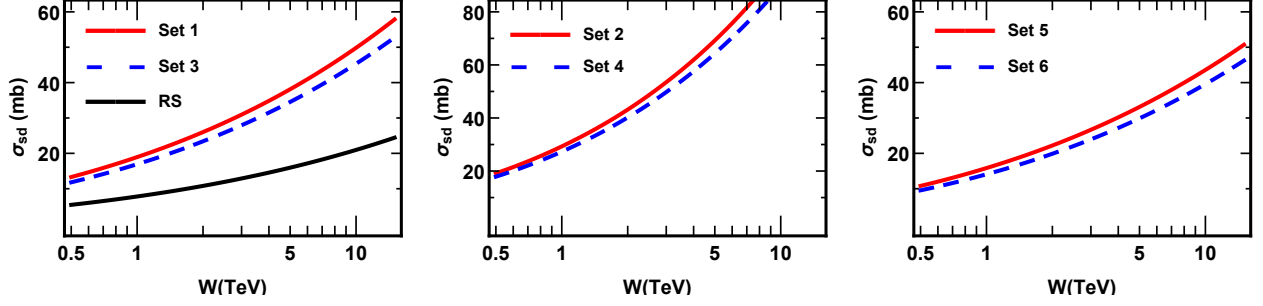


FIG. 12: Cross section of the single diffraction production $\int dy_M \frac{d\sigma_{sd}(Y, y_M)}{dy_M} = \sigma^{diff}$ versus Y for different sets of Ref. [74]. The solid black line, which is denoted by RS, corresponds to the saturation model of Ref. [70].

In Fig. 13 it shown the typical eikonal type shadowing corrections. [91], which suppress the large values of the diffraction cross section. The sum of the diagrams in Fig. 13 results in the following formula for $\frac{d\sigma_{sd}(Y, y_M)}{dy_M}$:

$$\frac{d\sigma_{sd}(Y, y_M)}{dy_M} = \int d^2b \, e^{-2N_p(Y, b)} \frac{d\sigma_{sd}(Y, y_M; b; Eq. (48))}{dy_M d^2b} \quad (47)$$

where

$$\begin{aligned} \frac{d\sigma_{sd}(Y, y_M; b)}{dy_M d^2b} &= \frac{2}{4\pi^2} \int d^2b' \int \frac{d^2r}{r^2} N_p(Y - y_M, \mathbf{r}, \mathbf{b} - \mathbf{b}') \\ &\times \left\{ \bar{\alpha}_S \int \frac{d^2r'}{2\pi} \frac{1}{r'^2} N_p\left(y_M, \mathbf{r}', \mathbf{b}' - \frac{1}{2}(\mathbf{r} - \mathbf{r}')\right) \frac{1}{(\mathbf{r} - \mathbf{r}')^2} N_p\left(y_M, \mathbf{r} - \mathbf{r}', \mathbf{b}' - \frac{1}{2}\mathbf{r}'\right) \right\} \end{aligned} \quad (48)$$

It should be noted that the shadowing corrections in Fig. 13 stems from the simple eikonal model as well as Eq. (35), and could be used only to show the scale of the effect. In particular, for $W = 13 TeV$ we evaluated $\sigma_{s.d.} = 4 mb$ indicating that the shadowing correction can be large.

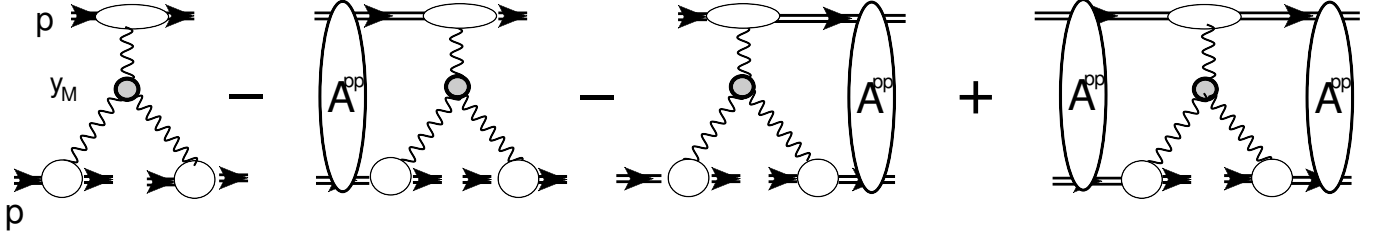


FIG. 13: Shadowing correction to the single diffraction production. $A^{pp}(Y, b)$ is given by Eq. (35).

The values for the cross section of diffractive production with the simplified shadowing correction of Eq. (47) are plotted in Fig. 14. One can see that the shadowing is very important, but the simple eikonal formula cannot pretend to take them all into account on the theoretical grounds. Again as for $\sigma_{tot}, \sigma_{el}$ and B_{el} , we see the need for the theoretical approach for the shadowing corrections. The experience with the simple models [9, 18, 29, 87–89] shows the eikonal formula can be used only as a rough estimate.

VII. CONCLUSIONS

In this paper we suggested a new approach to the structure of the soft Pomeron, based on the t -channel unitarity: we expressed the exchange of the soft Pomeron through the interaction of the dipole of small size on the order of

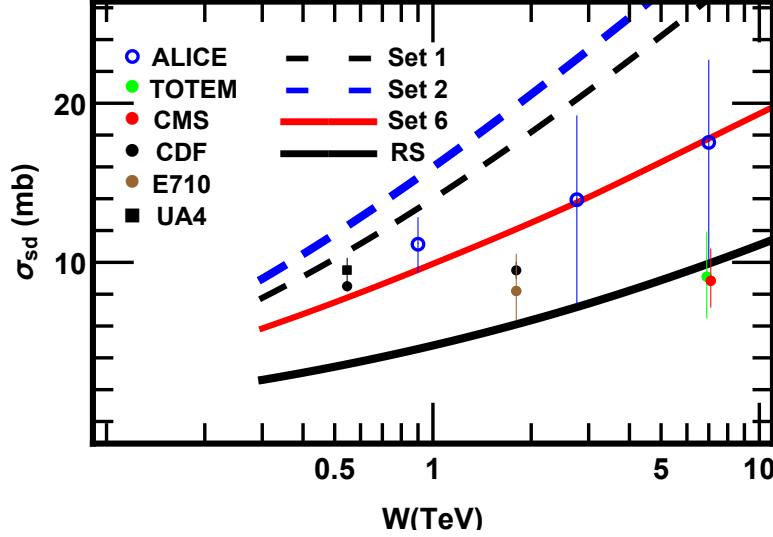


FIG. 14: The estimates for the single diffractive cross section using the simple eikonal formula of Eq. (47) for sets of parameters in Ref. [74] and for saturation model of Ref. [70](RS). The data are taken from Refs. [75, 92–94] .

$1/Q_s(Y)$ ($Q_s(Y)$ is the saturation momentum) with the hadrons. Thereby, it is shown that the typical distances in so called soft processes turns out to be small $r \sim 1/Q_s(\frac{1}{2}Y)$, where $Y = \ln s$. This fact opens new possibilities for describing the soft interactions in the framework of the Colour Glass Condensate(CGC) approach, putting the high energy phenomenology on solid theoretical basis.

The energy dependence of the scattering amplitude due to Pomeron exchange is determined by the saturation momentum $N_p^p(\mathbb{P}) \propto Q_s^2(\frac{1}{2}Y)$ (see Eq. (27)), which increases as a power of energy. Therefore, the suggested Pomeron leads to the violation of the Froissart theorem, but $N_p^p(\mathbb{P}) \propto Q_s^2(\frac{1}{2}Y) \propto e^{\lambda Y}$ with $\lambda \approx 0.1 - 0.13$ is in perfect agreement with phenomenological Donnachie-Landshoff Pomeron [47]. We believe, that our approach can be the good first approximation to start discussion of the soft process in CGC approach.

We made an attempt to describe the value of the Pomeron exchange directly from our knowledge of the deep inelastic processes. First off, we have to mention that we cannot describe DIS processes in framework of CGC in spite of the well known Balitsky-Kovchegov evolution equation. As we have discussed, B-K approach suffers from unsolved difficulties, including the large impact parameter (b) behaviour that violates the Froissart theorem [77–79]. We have to use models which introduce to B-K equation an additional exponential decrease at large b . Second, the models have been checked against the experimental data on DIS. However, the energy range of the experimental data are quite different from the one of soft interaction. The lesson, that we learned, is that some sets of parameterizations, which describe the DIS, lead to reasonable description of the soft high scattering but other sets cannot be described. In spite of the large dispersion of the estimates we see several general features, which could be useful in further development of the CGC approach to soft interaction. First, almost in all estimates we need strong shadowing corrections, both to obtain the reasonable values of the experimental observable, and to describe the shrinkage of the diffraction peak. The dressed Pomeron that we have introduced can not describe this shrinkage even on qualitative level. Second, the best description $\sigma_{tot}, \sigma_{el}, B_{el}$ and σ_{diff} we obtain from the impact parameter dependence that incorporates in the BFKL equation the Gribov's diffusion (see Refs. [85, 86] and references therein).

However, we can look on our attempts to obtain the soft Pomeron from the DIS saturation approach at a different angle, stating that sets 5 and 6 of Ref. [74] are good candidates for the global fit of DIS and soft interaction experimental data at high energies. The possibility of such combined description is both encouraging and exiting.

The approach, that we developed here, was started in Refs. [5, 9] for the exchange of the BFKL Pomeron, and it is the modified version of the MPSI treatment [8, 52], in which we use the properties of the BFKL Pomeron to absorb the QCD Born amplitude in the closed expression.

VIII. ACKNOWLEDGEMENTS

We thank our colleagues at Tel Aviv university and UTFSM for encouraging discussions. Part of this work has been done, while one of us (M.S.) has been visiting the Ohio State University, and he wishes to express his deep gratitude to Prof. Yu. Kovchegov for hospitality and help during this visit. This research was supported by ANID PIA/APOYO AFB180002 (Chile) and Fondecyt (Chile) grants 1180118 and 1191434, Conicyt Becas (Chile) and PIIC 009/2021, DPP, Universidad Tecnica Federico Santa Maria

* Electronic address: carlos.contreras@usm.cl

† Electronic address: leving@tauex.tau.ac.il, eugeniy.levin@usm.cl

‡ Electronic address: michael.sanhuezar@sansano.usm.cl

- [1] V. N. Gribov, “A Reggeon Diagram Technique,” Sov. Phys. JETP **26**, 414 (1968) [Zh. Eksp. Teor. Fiz. **53**, 654 (1967)]; “*Strong Interactions of Hadrons at High Energies*”. Cambridge, UK: Cambridge University Press, 2008. “*The theory of complex angular momenta: Gribov lectures on theoretical physics*,” Cambridge Monographs on Mathematical Physics Cambridge University Press 2003.
- [2] V. S. Fadin, E. A. Kuraev and L. N. Lipatov, “On the pomeron singularity in asymptotically free theories”, Phys. Lett. **B60**, 50 (1975); E. A. Kuraev, L. N. Lipatov and V. S. Fadin, “The Pomeron singularity in Nonabelian Gauge Theories” Sov. Phys. JETP **45**, 199 (1977), [Zh. Eksp. Teor. Fiz. **72**, 377 (1977)]; I. I. Balitsky and L. N. Lipatov, “The Pomeron singularity in Quantum Chromodynamics,” Sov. J. Nucl. Phys. **28**, 822 (1978), [Yad. Fiz. **28**, 1597 (1978)].
- [3] L. N. Lipatov, “The Bare Pomeron in Quantum Chromodynamics,” Sov. Phys. JETP **63**, 904 (1986) [Zh. Eksp. Teor. Fiz. **90**, 1536 (1986)].
- [4] L. N. Lipatov, “Small x physics in perturbative QCD,” Phys. Rept. **286** (1997), 131-198 [arXiv:hep-ph/9610276 [hep-ph]].
- [5] L. V. Gribov, E. M. Levin and M. G. Ryskin, “Semihard Processes in QCD,” Phys. Rept. **100**, 1 (1983).
- [6] E. M. Levin and M. G. Ryskin, “High-energy hadron collisions in QCD,” Phys. Rept. **189**, 267 (1990).
- [7] A. H. Mueller and J. Qiu, “Gluon recombination and shadowing at small values of x ”, Nucl. Phys. **B268** (1986) 427.
- [8] A. H. Mueller and B. Patel, “Single and double BFKL pomeron exchange and a dipole picture of high-energy hard processes”, Nucl. Phys. **B425** (1994) 471.
- [9] A. H. Mueller, “Soft gluons in the infinite momentum wave function and the BFKL pomeron,” Nucl. Phys. B **415** (1994) 373; “Unitarity and the BFKL pomeron,” Nucl. Phys. B **437** (1995) 107.
- [10] L. N. Lipatov, “High-energy scattering in QCD and in quantum gravity and two-dimensional field theories,” Nucl. Phys. B **365**, 614 (1991), “Gauge invariant effective action for high-energy processes in QCD,” Nucl. Phys. B **452**, 369 (1995), R. Kirschner, L. N. Lipatov and L. Szymanowski, “Effective action for multi - Regge processes in QCD,” Nucl. Phys. B **425**, 579 (1994), “Symmetry properties of the effective action for high-energy scattering in QCD,” Phys. Rev. D **51**, 838 (1995).
- [11] Y. V. Kovchegov and E. Levin, “Diffractive dissociation including multiple pomeron exchanges in high parton density QCD,” Nucl. Phys. B **577** (2000) 221, [hep-ph/9911523].
- [12] M. Braun, “Structure function of the nucleus in the perturbative QCD with $N_c \rightarrow \infty$ (BFKL pomeron fan diagrams),” Eur. Phys. J. C **16** (2000), 337-347 [arXiv:hep-ph/0001268 [hep-ph]]; M. A. Braun and G. P. Vacca, “Triple pomeron vertex in the limit $N_c \rightarrow \infty$,” Eur. Phys. J. C **6** (1999), 147-157 [arXiv:hep-ph/9711486 [hep-ph]]; J. Bartels, M. Braun and G. P. Vacca, “Pomeron vertices in perturbative QCD in diffractive scattering,” Eur. Phys. J. C **40**, 419 (2005); J. Bartels, L. N. Lipatov and G. P. Vacca, “Interactions of Reggeized gluons in the Moebius representation,” Nucl. Phys. B **706**, 391 (2005), [arXiv:hep-ph/0404110].
- [13] M. A. Braun, “Nucleus-nucleus scattering in perturbative QCD with $N_c \rightarrow \infty$ ”, Phys. Lett. B **483**, 115 (2000), [hep-ph/0003004]; “Nucleus nucleus interaction in the perturbative QCD,” Eur. Phys. J. C **33**, 113 (2004), [hep-ph/0309293]; “Conformal invariant pomeron interaction in the perturbative QCD with large N_c ,” Phys. Lett. B **632**, 297 (2006).
- [14] H. Navelet and R. B. Peschanski, “Conformal invariance and the exact solution of BFKL equations,” Nucl. Phys. B **507** (1997), 353-366 [arXiv:hep-ph/9703238 [hep-ph]].
- [15] J. Bartels, “Unitarity corrections to the Lipatov pomeron and the four gluon operator in deep inelastic scattering in QCD,” Z. Phys. C **60** (1993), 471-488 ; J. Bartels and M. Wusthoff, “The Triple Regge limit of diffractive dissociation in deep inelastic scattering,” Z. Phys. C **66** (1995), 157-180; J. Bartels and C. Ewerz, “Unitarity corrections in high-energy QCD,” JHEP **09** (1999), 026 [arXiv:hep-ph/9908454 [hep-ph]]; C. Ewerz, “Reggeization in high-energy QCD,” JHEP **0104** (2001) 031.
- [16] J. Bartels, “High-Energy Behavior In A Nonabelian Gauge Theory. 2. First Corrections To $T(N \rightarrow M)$ Beyond The Leading Lns Approximation,” Nucl. Phys. **B175**, 365 (1980); J. Kwiecinski and M. Praszalowicz, “Three Gluon Integral Equation And Odd C Singlet Regge Singularities In QCD,” Phys. Lett. **B94**, 413 (1980).
- [17] L. McLerran and R. Venugopalan, “Computing quark and gluon distribution functions for very large nuclei”, Phys. Rev. **D49** (1994) 2233, “Gluon distribution functions for very large nuclei at small transverse momentum”, Phys. Rev. **D49** (1994), 3352; “Green’s function in the color field of a large nucleus”, **D50** (1994) 2225; “Fock space distributions, structure

functions, higher twists, and small x , **D59** (1999) 09400.

- [18] A. H. Mueller and G. P. Salam, “*Large multiplicity fluctuations and saturation effects in onium collisions*,” Nucl. Phys. B **475**, 293 (1996), [hep-ph/9605302]; G. P. Salam, “*Studies of unitarity at small x using the dipole formulation*,” Nucl. Phys. B **461**, 512 (1996), [hep-ph/9509353].
- [19] I. Balitsky, “*Operator expansion for high-energy scattering*”, [arXiv:hep-ph/9509348]; “*Factorization and high-energy effective action*”, Phys. Rev. **D60**, 014020 (1999) [arXiv:hep-ph/9812311]; Y. V. Kovchegov, “*Small- x F_2 structure function of a nucleus including multiple Pomeron exchanges*” Phys. Rev. **D60**, 034008 (1999), [arXiv:hep-ph/9901281].
- [20] A. Kovner and M. Lublinsky, “*Odderon and seven Pomerons: QCD Reggeon field theory from JIMWLK evolution*,” JHEP **02** (2007), 058 [arXiv:hep-ph/0512316 [hep-ph]].
- [21] J. Jalilian-Marian, A. Kovner, A. Leonidov, and H. Weigert, “*The BFKL equation from the Wilson renormalization group*” , Nucl. Phys. **B504** (1997) 415–431, [arXiv:hep-ph/9701284].
- [22] J. Jalilian-Marian, A. Kovner, A. Leonidov, and H. Weigert, “*The Wilson renormalization group for low x physics: Towards the high density regime*” , Phys.Rev. **D59** (1998) 014014, [arXiv:hep-ph/9706377 [hep-ph]].
- [23] A. Kovner, J. G. Milhano, and H. Weigert, “*Relating different approaches to nonlinear QCD evolution at finite gluon density*” , Phys. Rev. **D62** (2000) 114005, [arXiv:hep-ph/0004014].
- [24] E. Iancu, A. Leonidov, and L. D. McLerran, *Nonlinear gluon evolution in the color glass condensate. I* ,Nucl. Phys. **A692** (2001) 583–645, [arXiv:hep-ph/0011241].
- [25] E. Iancu, A. Leonidov, and L. D. McLerran, “*The renormalization group equation for the color glass condensate*” , Phys. Lett. **B510** (2001) 133–144, [arXiv:hep-ph/0102009].
- [26] E. Ferreira, E. Iancu, A. Leonidov, and L. McLerran, “*Nonlinear gluon evolution in the color glass condensate. II*” , Nucl. Phys. **A703** (2002) 489–538, [arXiv:hep-ph/0109115].
- [27] H. Weigert, “*Unitarity at small Bjorken x* ,” Nucl. Phys. A **703** (2002), 823-860 [arXiv:hep-ph/0004044 [hep-ph]].
- [28] A. Kovner and J. G. Milhano, “*Vector potential versus color charge density in low x evolution*,” Phys. Rev. D **61** (2000), 014012 [arXiv:hep-ph/9904420 [hep-ph]].
- [29] T. Altinoluk, A. Kovner, E. Levin and M. Lublinsky, “*Reggeon Field Theory for Large Pomeron Loops*,” JHEP **04** (2014), 075 [arXiv:1401.7431 [hep-ph]].
- [30] A. Kovner and M. Lublinsky, “*In pursuit of Pomeron loops: The JIMWLK equation and the Wess-Zumino term*,” Phys. Rev. D **71** (2005), 085004 [arXiv:hep-ph/0501198 [hep-ph]].
- [31] A. Kovner and M. Lublinsky, “*From target to projectile and back again: Selfduality of high energy evolution*,” Phys. Rev. Lett. **94**, 181603 (2005), [hep-ph/0502119].
- [32] I. Balitsky, “*High-energy effective action from scattering of QCD shock waves*,” Phys. Rev. D **72**, 074027 (2005), arXiv:hep-ph/0507237.
- [33] Y. Hatta, E. Iancu, L. McLerran, A. Stasto and D. N. Triantafyllopoulos, “*Effective Hamiltonian for QCD evolution at high energy*,” Nucl. Phys. A **764**, 423 (2006), arXiv:hep-ph/0504182.
- [34] A. Kovner, M. Lublinsky and U. Wiedemann, “*From bubbles to foam: Dilute to dense evolution of hadronic wave function at high energy*,” JHEP **06** (2007), 075 [arXiv:0705.1713 [hep-ph]]; T. Altinoluk, A. Kovner, M. Lublinsky and J. Peressutti, “*QCD Reggeon Field Theory for every day: Pomeron loops included*,” JHEP **0903**, 109 (2009), [arXiv:0901.2559 [hep-ph]].
- [35] A. Kovner, E. Levin, M. Li and M. Lublinsky, “*Reggeon Field Theory and Self Duality: Making Ends Meet*,” JHEP **10** (2020), 185 [arXiv:2007.12132 [hep-ph]]; “*The JIMWLK evolution and the s-channel unitarity*,” JHEP **09** (2020), 199 [arXiv:2006.15126 [hep-ph]].
- [36] A. H. Mueller and A. I. Shoshi, “*Small x physics beyond the Kovchegov equation*,” Nucl. Phys. B **692**, 175 (2004), [hep-ph/0402193].
- [37] E. Iancu and D. N. Triantafyllopoulos, “*A Langevin equation for high energy evolution with pomeron loops*,” Nucl. Phys. A **756** (2005) 419, [hep-ph/0411405], “*Non-linear QCD evolution with improved triple-pomeron vertices*,” Phys. Lett. B **610** (2005) 253, [hep-ph/0501193]; E. Iancu, G. Soyez and D. N. Triantafyllopoulos, “*On the probabilistic interpretation of the evolution equations with Pomeron loops in QCD*,” Nucl. Phys. A **768** (2006) 194, [hep-ph/0510094].
- [38] A. H. Mueller, A. I. Shoshi and S. M. H. Wong, “*Extension of the JIMWLK equation in the low gluon density region*,” Nucl. Phys. B **715** (2005) 440.
- [39] E. Levin and M. Lublinsky, “*Balitsky’s hierarchy from Mueller’s dipole model and more about target correlations*,” Phys. Lett. B **607** (2005) 131, [hep-ph/0411121]; “*Towards a symmetric approach to high energy evolution: Generating functional with Pomeron loops*,” Nucl. Phys. A **763** (2005) 172, [hep-ph/0501173].
- [40] A. Kormilitzin, E. Levin and A. Prygarin, “*Multiparticle production in the mean field approximation of high density QCD*,” Nucl. Phys. A **813** (2008) 1, [arXiv:0807.3413 [hep-ph]].
- [41] E. Levin, J. Miller and A. Prygarin, “*Summing Pomeron loops in the dipole approach*,” Nucl. Phys. A **806** (2008) 245, [arXiv:0706.2944 [hep-ph]].
- [42] E. Levin, “*Dipole-dipole scattering in CGC/saturation approach at high energy: summing Pomeron loops*,” JHEP **1311** (2013) 039, [arXiv:1308.5052 [hep-ph]].
- [43] E. Gotsman, E. Levin and I. Potashnikova, “*CGC/saturation approach: secondary Reggeons and $\rho = \text{Re}/\text{Im}$ dependence on energy*,” Phys. Lett. B **786** (2018), 472-476 [arXiv:1807.06459 [hep-ph]].
- [44] V. A. Khoze, A. D. Martin and M. G. Ryskin, “*Dynamics of diffractive dissociation*,” Eur. Phys. J. C **81** (2021) no.2, 175 [arXiv:2012.07967 [hep-ph]].
- [45] K. J. Golec-Biernat and M. Wusthoff, “*Saturation in diffractive deep inelastic scattering*,” Phys. Rev. D **60** (1999) 114023 [hep-ph/9903358]; “*Saturation effects in deep inelastic scattering at low Q^2 and its implications on diffraction*,” Phys. Rev. D **59** (1998) 014017; [hep-ph/9807513].

- [46] A. Dumitru, D. E. Kharzeev, E. M. Levin and Y. Nara, “*Gluon Saturation in pA Collisions at the LHC: KLN Model Predictions For Hadron Multiplicities*,” Phys. Rev. C **85** (2012), 044920 [arXiv:1111.3031 [hep-ph]].
- [47] A. Donnachie and P. V. Landshoff, “*Elastic Scattering and Diffraction Dissociation*,” Nucl. Phys. B **244** (1984), 322
- [48] M. Froissart, “*Asymptotic Behavior and Subtractions in the Mandelstam Representation*,” Phys. Rev. **123** (1961) 1053; A. Martin, “*Scattering Theory: Unitarity, Analyticity and Crossing*,” Lecture Notes in Physics, Springer-Verlag, Berlin-Heidelberg-New-York, 1969.
- [49] R. J. Glauber and G. Matthiae, “*High-energy scattering of protons by nuclei*,” Nucl. Phys. B **21** (1970), 135-157.
- [50] I. Gradshteyn and I. Ryzhik, *Table of Integrals, Series, and Products*, Fifth Edition, Academic Press, London, 1994.
- [51] Yuri V. Kovchegov and Eugene Levin, “*Quantum Chromodynamics at High Energies*”, Cambridge Monographs on Particle Physics, Nuclear Physics and Cosmology, Cambridge University Press, 2012 .
- [52] A. H. Mueller and G. Salam, “*Large multiplicity fluctuations and saturation effects in onium collisions*,” Nucl. Phys. B **475** (1996), 293-320 [arXiv:hep-ph/9605302 [hep-ph]]; G. Salam, “*Studies of unitarity at small x using the dipole formulation*,” Nucl. Phys. B **461** (1996), 512-538 [arXiv:hep-ph/9509353 [hep-ph]]; E. Iancu and A. Mueller, “*Rare fluctuations and the high-energy limit of the S matrix in QCD*,” Nucl. Phys. A **730** (2004), 494-513 [arXiv:hep-ph/0309276 [hep-ph]]; “*From color glass to color dipoles in high-energy onium onium scattering*,” Nucl. Phys. A **730** (2004), 460-493 [arXiv:hep-ph/0308315 [hep-ph]].
- [53] Y. V. Kovchegov, “*Inclusive gluon production in high energy onium-onium scattering*,” Phys. Rev. D **72** (2005), 094009, [arXiv:hep-ph/0508276 [hep-ph]].
- [54] E. Levin, “*High energy amplitude in the dipole approach with Pomeron loops: Asymptotic solution*,” Nucl. Phys. A **763** (2005), 140-171, [arXiv:hep-ph/0502243 [hep-ph]].
- [55] A. H. Mueller and D. N. Triantafyllopoulos, “*The Energy dependence of the saturation momentum*,” Nucl. Phys. B **640** (2002) 331 [hep-ph/0205167].
- [56] J. Bartels, K. J. Golec-Biernat and H. Kowalski, “*A modification of the saturation model: DGLAP evolution*,” Phys. Rev. D **66** (2002) 014001 [hep-ph/0203258].
- [57] H. Kowalski and D. Teaney, “*An Impact parameter dipole saturation model*,” Phys. Rev. D **68** (2003) 114005 [hep-ph/0304189].
- [58] E. Iancu, K. Itakura and S. Munier, “*Saturation and BFKL dynamics in the HERA data at small x*,” Phys. Lett. B **590** (2004) 199 [hep-ph/0310338].
- [59] H. Kowalski, L. Motyka and G. Watt, “*Exclusive diffractive processes at HERA within the dipole picture*,” Phys. Rev. D **74** (2006) 074016 [hep-ph/0606272].
- [60] H. Kowalski, T. Lappi and R. Venugopalan, “*Nuclear enhancement of universal dynamics of high parton densities*,” Phys. Rev. Lett. **100** (2008) 022303 [arXiv:0705.3047 [hep-ph]].
- [61] H. Kowalski, T. Lappi, C. Marquet and R. Venugopalan, “*Nuclear enhancement and suppression of diffractive structure functions at high energies*,” Phys. Rev. C **78** (2008) 045201 [arXiv:0805.4071 [hep-ph]].
- [62] G. Watt and H. Kowalski, “*Impact parameter dependent colour glass condensate dipole model*,” Phys. Rev. D **78** (2008) 014016 [arXiv:0712.2670 [hep-ph]].
- [63] A. H. Rezaeian, “*CGC predictions for p+A collisions at the LHC and signature of QCD saturation*,” Phys. Lett. B **718** (2013) 1058 [arXiv:1210.2385 [hep-ph]].
- [64] J. L. Albacete, N. Armesto, J. G. Milhano, P. Quiroga-Arias and C. A. Salgado, “*AAMQS: A non-linear QCD analysis of new HERA data at small-x including heavy quarks*,” Eur. Phys. J. C **71** (2011), 1705, [arXiv:1012.4408 [hep-ph]] and reference therein.
- [65] T. Lappi and H. Mantysaari, “*Incoherent diffractive J/Psi-production in high energy nuclear DIS*,” Phys. Rev. C **83** (2011) 065202 [arXiv:1011.1988 [hep-ph]].
- [66] T. Toll and T. Ullrich, “*Exclusive diffractive processes in electron-ion collisions*,” Phys. Rev. C **87** (2013) 2, 024913 [arXiv:1211.3048 [hep-ph]].
- [67] P. Tribedy and R. Venugopalan, “*Saturation models of HERA DIS data and inclusive hadron distributions in p+p collisions at the LHC*,” Nucl. Phys. A **850** (2011) 136 [Nucl. Phys. A **859** (2011) 185] [arXiv:1011.1895 [hep-ph]].
- [68] P. Tribedy and R. Venugopalan, “*QCD saturation at the LHC: comparisons of models to p+p and A+A data and predictions for p+Pb collisions*,” Phys. Lett. B **710** (2012) 125 [Phys. Lett. B **718** (2013) 1154] [arXiv:1112.2445 [hep-ph]].
- [69] A. H. Rezaeian, M. Siddikov, M. Van de Klundert and R. Venugopalan, “*IP-Sat: Impact-Parameter dependent Saturation model revised*,” PoS DIS **2013** (2013) 060 [arXiv:1307.0165 [hep-ph]]; “*Analysis of combined HERA data in the Impact-Parameter dependent Saturation model*,” Phys. Rev. D **87** (2013) 3, 034002 [arXiv:1212.2974].
- [70] A. H. Rezaeian and I. Schmidt, “*Impact-parameter dependent Color Glass Condensate dipole model and new combined HERA data*,” Phys. Rev. D **88** (2013) 074016 [arXiv:1307.0825 [hep-ph]].
- [71] C. Contreras, E. Levin and I. Potashnikova, “*CGC/saturation approach: a new impact-parameter dependent model*,” Nucl. Phys. A **948** (2016), 1-18 [arXiv:1508.02544 [hep-ph]].
- [72] C. Contreras, E. Levin, R. Meneses and I. Potashnikova, “*CGC/saturation approach: a new impact-parameter dependent model in the next-to-leading order of perturbative QCD*,” Phys. Rev. D **94** (2016) no.11, 114028 [arXiv:1607.00832 [hep-ph]].
- [73] B. Ducloe, E. Iancu, A. H. Mueller, G. Soyez and D. N. Triantafyllopoulos, “*Non-linear evolution in QCD at high-energy beyond leading order*,” JHEP **1904** (2019) 081 [arXiv:1902.06637 [hep-ph]] and references therein.
- [74] C. Contreras, E. Levin and M. Sanhueza, “*Non-linear evolution in the re-summed next-to-leading order of perturbative QCD: confronting the experimental data*,” [arXiv:2106.06214 [hep-ph]].
- [75] The Review of Particle Physics (2018), M. Tanabashi et al. (Particle Data Group), Phys. Rev. D **98**, 030001 (2018).
- [76] G. Antchev et al. [TOTEM Collaboration], “*First measurement of elastic, inelastic and total cross-section at $\sqrt{s} = 13$ TeV*

- by TOTEM and overview of cross-section data at LHC energies,” Eur. Phys. J. C **79** (2019) no.2, 103, [arXiv:1712.06153 [hep-ex]].
- [77] A. Kovner and U. A. Wiedemann, “Nonlinear QCD evolution: Saturation without unitarization,” Phys. Rev. D **66**, 051502 (2002) [hep-ph/0112140].
 - [78] A. Kovner and U. A. Wiedemann, “Perturbative saturation and the soft pomeron,” Phys. Rev. D **66**, 034031 (2002) [hep-ph/0204277]; ;
 - [79] A. Kovner and U. A. Wiedemann, “No Froissart bound from gluon saturation,” Phys. Lett. B **551**, 311 (2003) [hep-ph/0207335].
 - [80] E. Ferreiro, E. Iancu, K. Itakura and L. McLerran, “Froissart bound from gluon saturation,” Nucl. Phys. A **710**, 373 (2002) [hep-ph/0206241].
 - [81] J. Bartels, E. Levin, “Solutions to the Gribov-Levin-Ryskin equation in the nonperturbative region,” Nucl. Phys. **B387** (1992) 617-637;]
 - [82] E. Iancu, K. Itakura and L. McLerran, “Geometric scaling above the saturation scale,” Nucl. Phys. A **708** (2002) 327 [hep-ph/0203137].
 - [83] A. M. Stasto, K. J. Golec-Biernat, J. Kwiecinski, “Geometric scaling for the total $\gamma^* p$ cross-section in the low x region,” Phys. Rev. Lett. **86** (2001) 596-599, [hep-ph/0007192].
 - [84] C. Contreras, E. Levin, R. Meneses and M. Sanhueza, “Non-linear equation in the re-summed next-to-leading order of perturbative QCD: the leading twist approximation,” Eur. Phys. J. C **80** (2020) no.11, 1029 [arXiv:2007.06214 [hep-ph]].
 - [85] E. Levin, “Large b behaviour in the CGC/saturation approach: BFKL equation with pion loops,” Phys. Rev. D **91** (2015) no.5, 054007 [arXiv:1412.0893 [hep-ph]].
 - [86] E. Gotsman and E. Levin, “Large impact parameter behavior in the CGC/saturation approach: A new nonlinear equation,” Phys. Rev. D **101** (2020) no.1, 014023 [arXiv:1910.11662 [hep-ph]].
 - [87] E. Levin and M. Lublinsky, “A Linear evolution for nonlinear dynamics and correlations in realistic nuclei,” Nucl. Phys. A **730** (2004), 191-211, [arXiv:hep-ph/0308279 [hep-ph]].
 - [88] E. Levin and M. Lublinsky, “Balitsky’s hierarchy from Mueller’s dipole model and more about target correlations,” Phys. Lett. B **607** (2005), 131-138, [arXiv:hep-ph/0411121 [hep-ph]].
 - [89] J. P. Blaizot, E. Iancu and D. N. Triantafyllopoulos, “A Zero-dimensional model for high-energy scattering in QCD,” Nucl. Phys. A **784** (2007), 227-258, [arXiv:hep-ph/0606253 [hep-ph]].
 - [90] E. Gotsman, E. Levin and I. Potashnikova, “CGC/saturation approach: soft interaction at the LHC energies,” Phys. Lett. B **781** (2018), 155-160, [arXiv:1712.06992 [hep-ph]].
 - [91] E. Gotsman, E. Levin and U. Maor, “Diffractive dissociation and eikonalization in high-energy pp and p anti- p collisions,” Phys. Rev. D **49** (1994), R4321-R4325, [arXiv:hep-ph/9310257 [hep-ph]].
 - [92] J. Kaspar, “Soft diffraction at LHC”, EPJ Web of Conference **72** , 06005(2018), <https://doi.org/10.105/epjconf/2018172060005>.
 - [93] B. Abelev *et al.* [ALICE], “Measurement of inelastic, single- and double-diffraction cross sections in proton–proton collisions at the LHC with ALICE,” Eur. Phys. J. C **73** (2013) no.6, 2456, [arXiv:1208.4968 [hep-ex]].
 - [94] V. Khachatryan *et al.* [CMS], “Measurement of diffraction dissociation cross sections in pp collisions at $\sqrt{s} = 7$ TeV,” Phys. Rev. D **92** (2015) no.1, 012003, [arXiv:1503.08689 [hep-ex]].